Available online at www.sciencedirect.com
SCIENCE DIRECT®
Journal of Organometallic Chemistry 690 (2005) 57–68
Journal of Organometallic Chemistry
www.elsevier.com/locate/jorganchem

The effect of carbon chain length of the diphosphine ligand on the aurophilic interaction. Synthesis and X-ray structural study for a series of Au(I) compounds with Ph_2P–R–PPh_2 and S-$(CH_2)_n$-py ligands

Satoru Onaka [a,*], Masanobu Yaguchi [a], Ryuichiro Yamauchi [a], Tomoji Ozeki [b], Mitsuhiro Ito [a], Tetsuya Sunahara [a], Yukako Sugiura [a], Michito Shiotsuka [c], Keiko Nunokawa [a], Makoto Horibe [a], Kazuya Okazaki [a], Akifumi Iida [b], Hirokazu Chiba [b], Katsuya Inoue [d], Hiroyuki Imai [d], Katsuya Sako [c]

[a] *Department of Environmental Technology, Graduate School of Engineering, Nagoya Institute of Technology, Gokiso-cho, Showa-ku, Nagoya 466-8555, Japan*
[b] *Department of Chemistry and Materials Science, Tokyo Institute of Technology, 2-12-1 Ookayama, Meguro-ku, Tokyo 152-8551, Japan*
[c] *Department of Systems Management and Engineering, Nagoya Institute of Technology, Showa-ku, Nagoya 466-8555, Japan*
[d] *Institute for Molecular Science, Myodaiji, Okazaki 444-8484, Japan*

Received 8 June 2004; accepted 18 August 2004
Available online 25 September 2004

Abstract

The effect of the carbon chain-length for Ph_2P–R–PPh_2 (R = –CH=CH–, $–CH_2–CH_2–$, $–CH_2–CH_2–CH_2–$, and $–CH_2–CH_2–CH_2–$ $CH_2–$) and S-$(CH_2)_n$-pyridine ligand (n = 0 to 2) on the aurophilic interaction has been explored systematically. The effect of the N position in x-mercaptopyridine (x = 2 or 4) toward Au(I) center and/or the SR group was also investigated. X-ray structural study was made for 12 new derivatives. The Au–Au distances are below 3.0 Å for 2-S-pyridine derivatives with Ph_2P–CH=CH–PPh_2 (t-dpen) and $Ph_2P–CH_2–CH_2–PPh_2$ (dppe) ligand and the pyridine N atoms come in close contact with the H atoms of these diphosphine carbon chains. A local coplanar conformation is formed between 2-S-pyridine and Au–P–CH groups for these derivatives. The carbon chain lengths are not too consequential on the induction of aurophilicity. Various infinite and/or dimer structures have been revealed from single crystal X-ray analysis for the present series of compounds.

Keywords: Aurophilicity; Pyridinethiol; Diphosphine; N–H interaction; Infinite chains

1. Introduction

The use of aurophilic interaction is a sophisticated strategy to construct supra molecules and nanometer-sized molecules on a gold(I) derivative as a scaffolding [1–3]. However, there have been many debates on the factors which are important to the appearance and the strength of the aurophilic interaction. For instance, the steric effect of ligands and/or the crystal packing force are sometimes more accentuated than the electronic effect of ligands or vice versa [4–10]. Pykkö et al. [11] have highlighted the importance of the steric effect of the SR group from their theoretical calculations. Substitution of a SR (R = organic group) group for X in $XAuPR'_3$ compounds is a well-known stratagem to induce and/

* Corresponding author. Tel.: +81527355160; fax: +8152735516.
E-mail address: onaka.satoru@nitech.ac.jp (S. Onaka).

0022-328X/$ - see front matter © 2004 Elsevier B.V. All rights reserved.
doi:10.1016/j.jorganchem.2004.08.028

or reinforce the aurophilicity of this type of Au(I) derivatives [11]. Balch et al. [12] have made a systematic study for a series of $(Au–X)_2(\mu_2\text{-}PPh_2–(CH_2)_n–PPh_2)$ (n = 4 to 8) derivatives and pointed out that Au–Au distances do not depend simply on the length of the carbon chains, but the woven structure by the carbon backbone is largely influential. We have shown that the advent of aurophilicity depends on the intricate balance among crystal packing force, steric demands of the phosphine ligand, and the interaction ($\tilde{\pi}$-π stack) between aromatic rings for a series of $(m\text{-}CF_3–C_6H_4)_3P–Au–X$ derivatives (X = Cl, SR) in the previous paper [13]. The previous paper has also shown that the aurophilicity is weakend for 4-*S*-pyridyl derivatives than for the *S*-phenyl derivatives [13]. This finding has led us to assess the influence of the S position in the pyridine-thiolate ligand on the aurophilicity for [Au(*x*-*S*-pyridine)]$_2$(μ-diphos) type derivatives (x = 2 and/or 4). The first onset of this study was made for [Au(2-*S*-pyridine)]$_2$(μ_2-*t*-dpen) (**1**) (*t*-dpen = *trans*-1,2-bis (diphenyl phosphino) ethylene). Single crystal X-ray analysis on **1** has revealed two interesting results; a short Au–Au distance and significant pyridine-N···H–C (ethylene) contact, indicative of a hydrogen bond. These serendipitous findings have enticed us to systematic exploration on [Au(*x*-*S*-pyridine)]$_2$(μ_2-*t*-dpen). The present study was undertaken to glean essential ingredients by changing the length of carbon chain in the diphosphine and/or pyridine-thiolate ligands and the S-position, by which the rational design and the fabrication of extended gold-based molecular assemblies will be possible.

2. Results

2.1. Synthesis

The new diphosphine-bridged gold arylthiol complexes $(AuSR)_2(\mu\text{-}Ph_2P–C_n–PPh_2)$ (n = 2 to 4), **1**–**10**, were synthesized by the reaction of $(AuCl)_2(\mu\text{-}Ph_2P–C_n–PPh_2)$ with two equivalent amounts of HSR together with KOH or Na_2CO_3 in CH_2Cl_2/CH_3OH. Au{4-*S*-$(CH_2)_n$-pyridines}PPh_3, **11** and **12**, were similarly synthesized from $Au(Cl)PPh_3$ with 4-HS-$(CH_2)_n$-pyridine (1:1 ratio) together with KOH in CH_2Cl_2/CH_3OH. All these compounds were obtained in a satisfactory yield. The ^{1}H NMR spectrum of each compound supports the synthesis of new respective gold-thiol derivatives, which was confirmed by single crystal X-ray analysis. The ^{31}P NMR spectra in $CDCl_3$ exhibit a singlet (ca. 36 ppm) at room temperature for the present series of SR complexes. Substitution of the SR group for Cl in the precursor diphosphine Au chlorides induces a considerable lower-filed shift compared with a singlet at ca. 30 ppm for each parental chloride. The trend is consistent with our previous observations [13–15]. Thus, each of solid-state molecular structures appears to exist in solutions at room temperature.

2.2. Molecular structures

The molecular structures of **1**–**5** which are composed of P–C═C–P and P–C–C–P skeletons are quite similar except the tilt of the SR ring (Figs. 1(a)–5(a)). The crystals **1**, **2** and **3** belong to the monoclinic system 2/*m* (*C*2/c, *P*21/*n* and *C*2/*c*, respectively), while **4** and **5** belong to the triclinic system, $\bar{P}$. The predominant molecular shape for **1**–**5** has a sinusoidal S–Au–P–P–Au–S skeleton in which the SR groups are oriented to an opposite direction for each other. There are two independent molecules in a unit cell of **5**; only one molecule is shown in Fig. 5(a). The center of symmetry is located at the midst of the C═C backbone for **1**. Similarly, there is a center of symmetry at the midst of the C–C backbone for **3**, **4** and each molecule of **5**. For the diphosphine with a P–C–C–C–P backbone, single crystals were obtained for the 2-*S*-pyridine and SPh derivatives **6** and **7**. X-ray structure analysis shows a sinusoid chain structure (Figs. 6(a) and 7(a)). The C–C–C-chains of **6** and **7** exhibit an elongated C–C–C form and the bent direction of the two Au-2-*S*-py groups is opposite in **6**. Three kind of substitution products **8**–**10** were synthe-

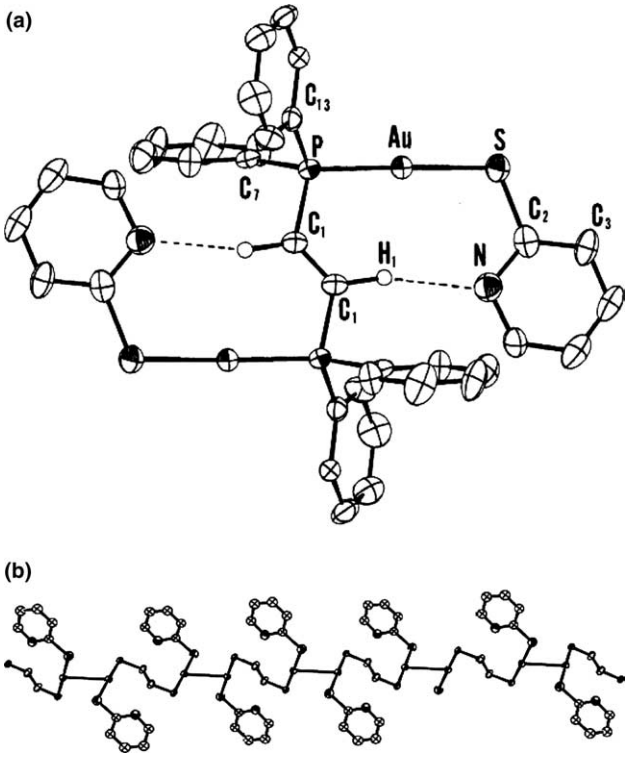

Fig. 1. (a) An ORTEP drawing of (2-*S*-pyridine-Au)$_2$(μ_2-*t*-dpen) (**1**). (b) Infinites chains composed of aurophilicity for **1**. The chains are almost in the *ac* plane.

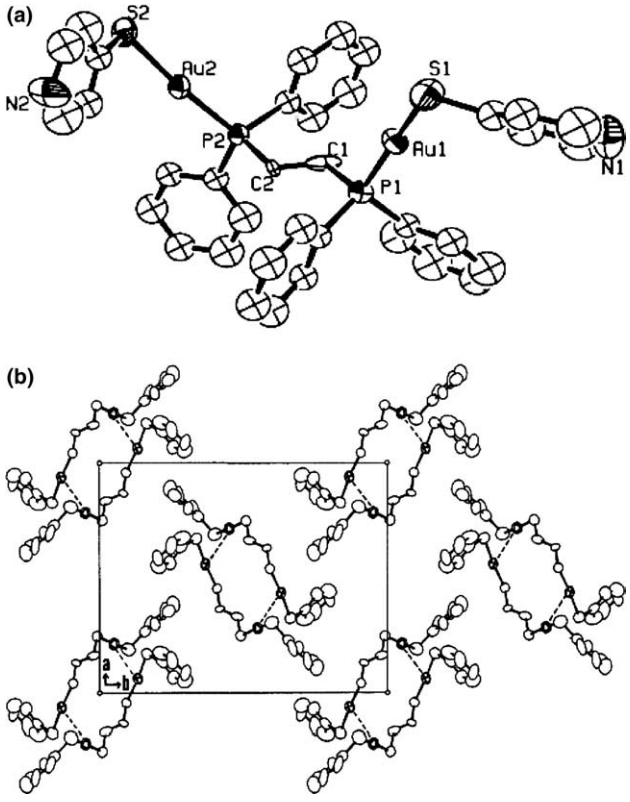

Fig. 2. (a) An ORTEP drawing of (4-*S*-pyridine-Au)$_2$(μ_2-*t*-dpen) (**2**). (b) The molecular packing of **2** along the *c*-axis, which shows dimer formation through aurophilicity interaction. Phenyl groups are omitted for clarity.

sized for the P–C–C–C–C–P diphosphine ligand. All three these compounds were obtained in a form of single crystals (Figs. 8(a)–10(a)). The C–C–C–C-chain of **8**, which possesses the 2-*S*-py ligand as an SR group exhibits an elongated C–C–C–C form and the bent direction of the two Au-2-*S*-py groups is opposite in **8**. The molecular structure of **9** which possesses the 4-*S*-py ligand is composed of a rectangular C–C–C–C backbone. Two independent molecules with distinctly different conformations relevant to the –C–C–C–C– backbone are contained in a unit cell of **10** in which the SPh substitutes for Spy ligands in **8** and **9**. The methylene groups in the hydrocarbon chain and the phosphorus atoms have anti, staggered conformations similar to that depicted in Fig. 10(a) for one molecule of **10**; in another molecule, the CH_2 groups and the phosphorus atoms have rectangular, staggered conformations similar to that illustrated in Fig. 9(a) and the two inside CH_2 groups occupy disordered positions pointed to an opposite direction. Although **8**–**10** possess the four hydrocarbon chain in the diphosphine ligand, the vectors of the two S–Au–P groups for these molecules are significantly different; the vectors are almost reversed for **8** and **10**, while the angle between these vectors is loosened significantly from 180° for the 4-*S*-pyridine derivative **9**.

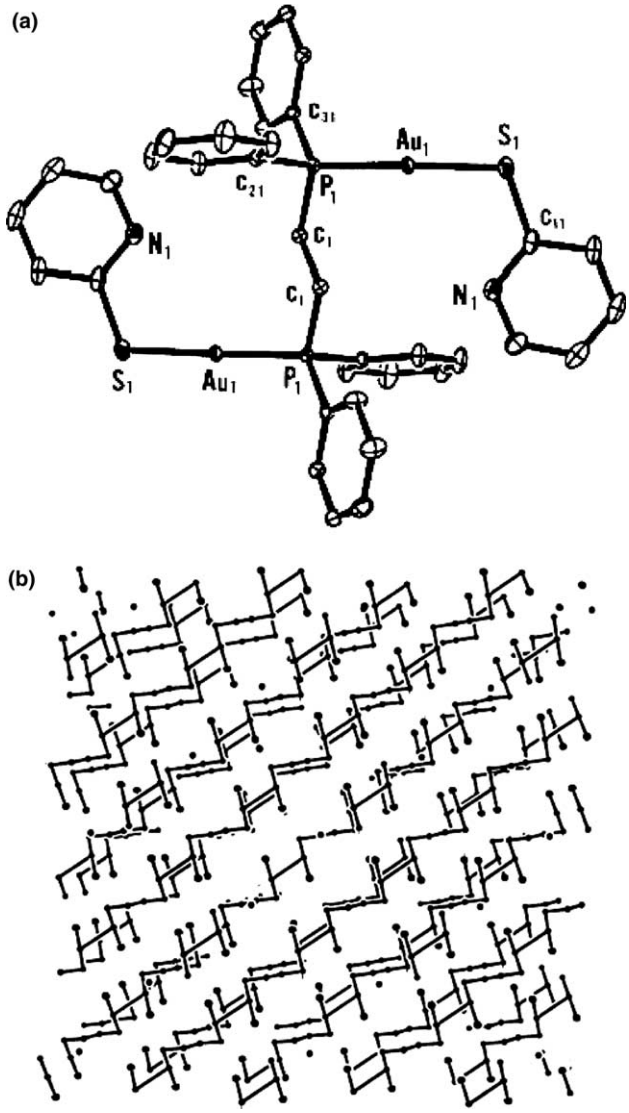

Fig. 3. (a) An ORTEP drawing of (2-*S*-pyridine-Au)$_2$(μ_2-dppe) (**3**). (b) Infinites chains composed of aurophilicity for **3**. Phenyl groups are omitted for clarity.

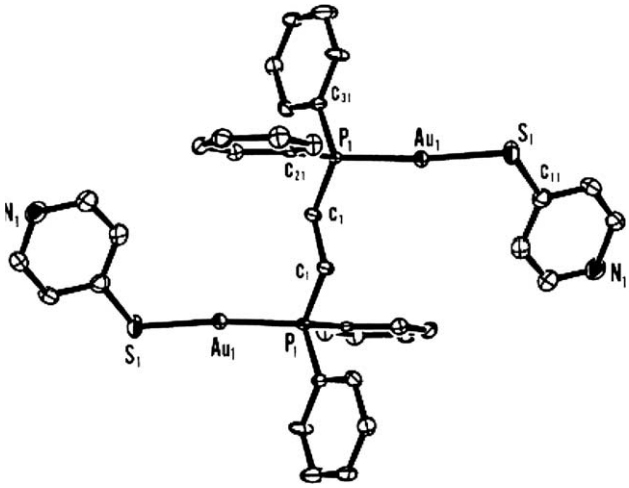

Fig. 4. An ORTEP drawing of (4-*S*-pyridine-Au)$_2$(μ_2-dppe) (**4**).

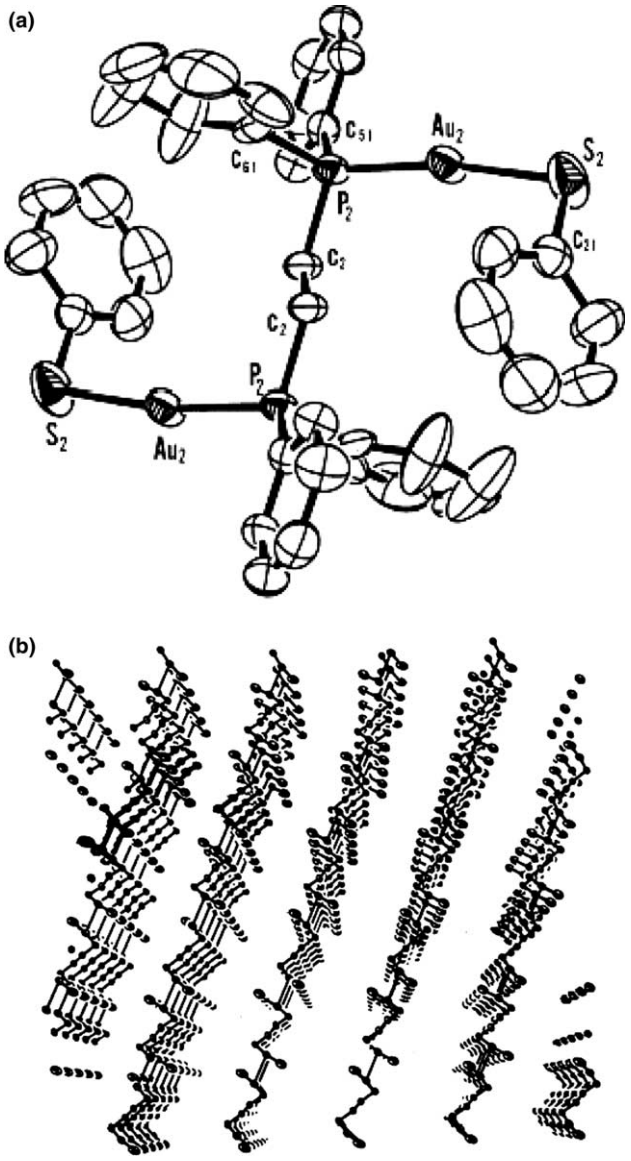

Fig. 5. (a) An ORTEP drawing of (S-Ph-Au)$_2$(μ_2-dppe) (**5**). (b) Infinite chains composed of aurophilicity and the dppe ligand for **5**, viewed down along the *a*-axis.

In order to assess the effect of the carbon chain length in *S*-$(CH_2)_n$-py ligand on the conformation of molecules, Au(4-*S*-CH_2-py)PPh_3 (**11**), and Au{4-*S*-$(CH_2)_2$-py}PPh_3 (**12**) were synthesized and subjected to single crystal X-ray diffraction analysis. The structures of these molecules are shown in Figs. 11 (**11**) and 12 (**12**). Compounds **11** and **12** exist as an isolated molecule in solid states. An interesting structural feature of **12** is that the S–C–C–C(py) backbone is bent back to the Ph_3P–Au moiety.

Selected bond lengths and angles are collected in Table 2. As three different kinds of diffractometers were used to collect the diffraction data and the quality of data are not at the same level, it seems better to avoid precise metrical comparisons among these parameters

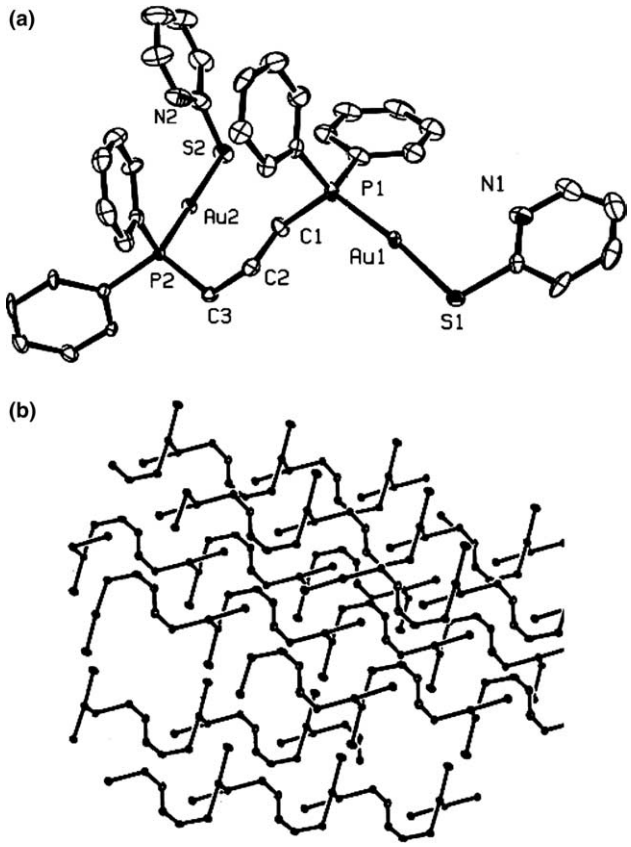

Fig. 6. (a) An ORTEP drawing of (2-*S*-pyridine-Au)$_2$(μ_2-dppp) (**6**). (b) Infinite chains composed of aurophilicity and the dppp ligand for **6**, which is almost parallel to the *a*-axis.

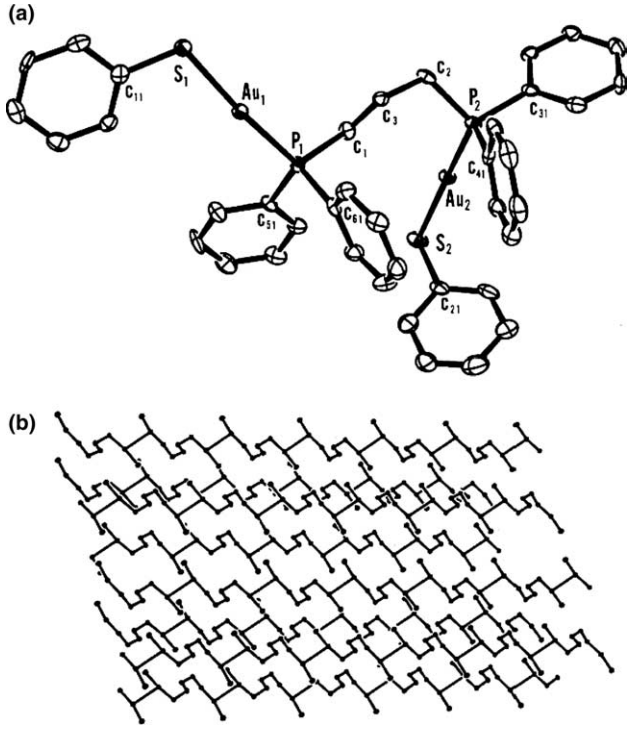

Fig. 7. (a) An ORTEP drawing of (*S*-phenyl-Au)$_2$(μ_2-dppp) (**7**). (b) Infinite chains composed of aurophilicity and the dppp ligand for **7**, viewed down along the *b*-axis.

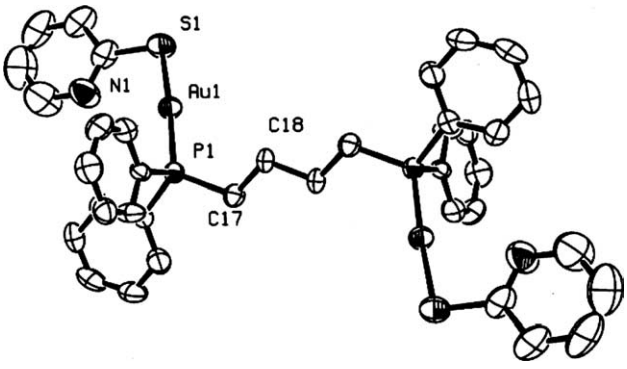

Fig. 8. An ORTEP drawing of (2-*S*-pyridine-Au)$_2$(μ_2-dppb) (**8**).

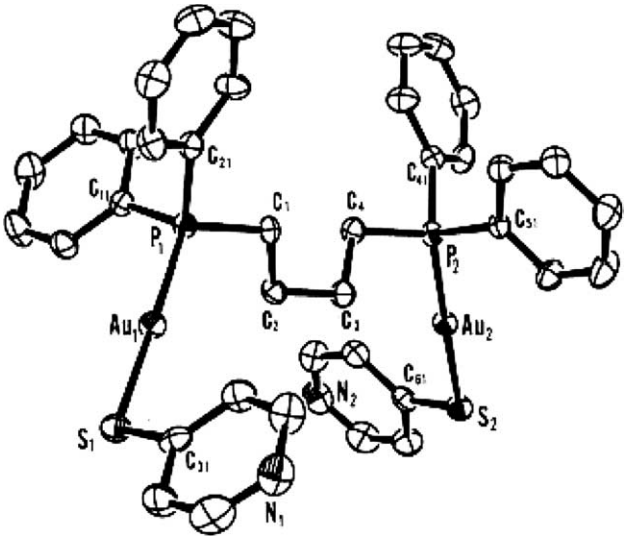

Fig. 9. An ORTEP drawing of (4-*S*-pyridine-Au)$_2$(μ_2-dppb) (**9**).

except discussions on trends for these derivatives. For RS–Au–P⁀P–Au–SR series, Au–S and Au–P distances fall within normal ranges (ca. 2.31 and 2.26 Å, respectively) [13–15]. There is no apparent changes of these lengths along with the elongation of the carbon backbone. The P–Au–S bond angles are almost linear and there appears no systematic changes with the change of the carbon backbone; those angles for **7** are the most acute (167.63(6)° and 171.26(6)°). The Au–S–C(*ipso*) angles are around 109°. There is also no systematic changes of these angles with the changes of the carbon chain.

3. Discussions

3.1. Crystal structures and aurophilicity

Systematic exploration of the substitution effect of X group and/or diphosphine on the aurophilic interaction has been made for (AuX)$_2$(diphos)-type compounds described above (X = 2-*S*-py, 4-*S*-py and *S*-Ph). Typical solid-state structural motifs for (AuX)$_2$diphos so far known are classified into four types A, B, C, and D and are summarized in Chart 1; there is no Au–Au interaction in D. The motifs of **1**–**10** are A, B, A, D, A, A, A, D, (A) and A, respectively. Among the crystal packing diagrams for aforementioned molecules, only archetypal cases for aurophilic interaction are shown in Fig. 1(b)–3(b) and 5(b)–7(b) for **1**–**3**, and **5**–**7**. Compounds **1** and **3** indicate a strong Au–Au interaction

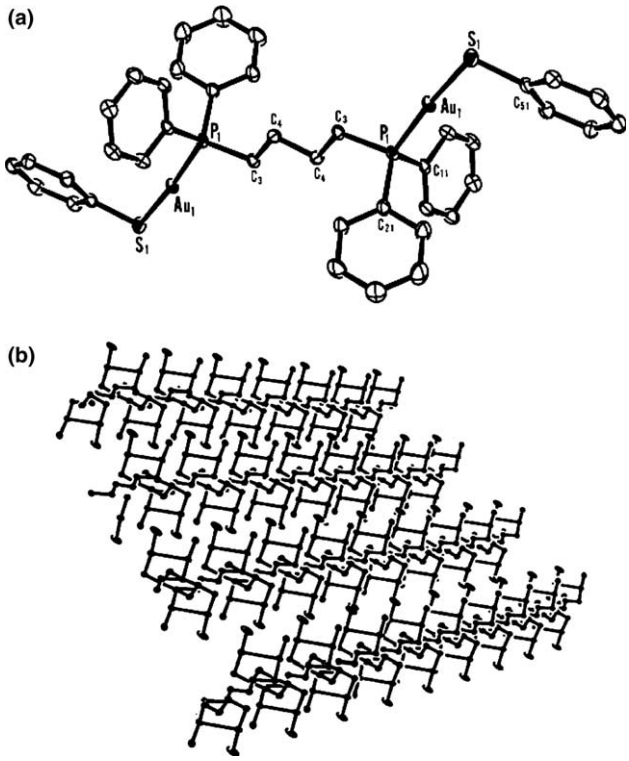

Fig. 10. (a) An ORTEP drawing of (*S*-phenyl-Au)$_2$(μ_2-dppb) (**10**). (b) Infinite chains composed of aurophilicity and the dppb ligand for **10**, viewed down along the *c*-axis.

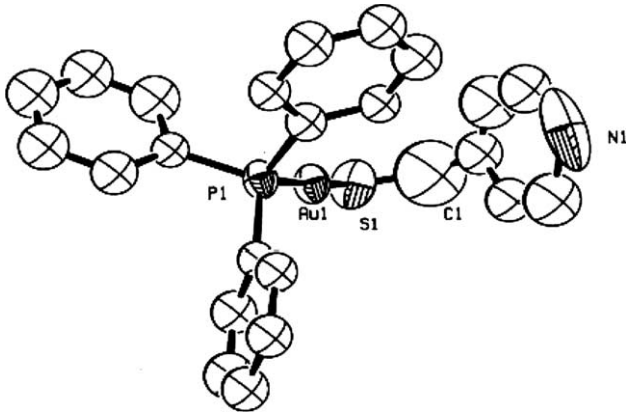

Fig. 11. An ORTEP drawing of Au (4-*S*-CH$_2$-pyridine)(PPh$_3$) (**11**).

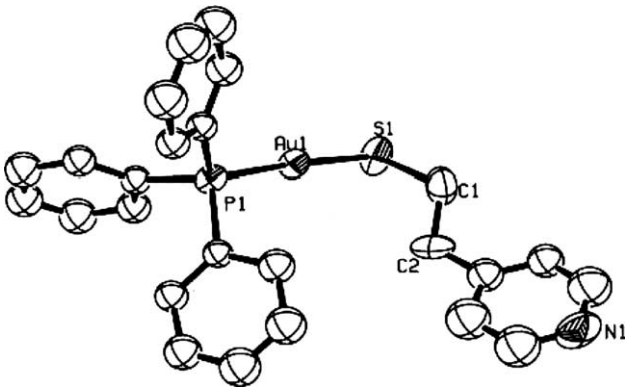

Fig. 12. An ORTEP drawing of Au (4-*S*-CH_2-CH_2-pyridine)(PPh_3) (**12**).

(r(Au–Au) = 2.986(1) and 2.9679(2) Å for **1** and **3**, respectively) and a quasi one-dimensional infinite chain is thus formed (Figs. 1(b) and 3(b)). By substituting 4-*S*-pyridyl groups for 2-*S*-pyridyl groups in **1**, the N-position isomer **2** is obtained. The Au–Au distance in **2** is significantly elongated (r(Au–Au) = 3.239(2) Å) and dimers are formed via two Au(I) centers in one molecule which is connected to an adjacent molecule of **2** (Fig. 2(b)). Compound **4** is formed upon substitution of 4-*S*-pyridyl groups for 2-*S*-pyridyl groups in **3**. The Au–Au interaction is amazingly elongated from r(Au–Au) = 2.9679(2) to 5.8749(7) Å by this substitution; this distance is far beyond the Au–Au interaction. By substituting phenyl groups for 2-*S*-pyridyl groups in **1** and **3**, $(AuSPh)_2(\mu_2$-*t*-dpen) [14] and the *S*-Ph analogue **5** (dppe backbone) are obtained. For both of them, quasi one-dimensional infinite chains are formed; the chain of **5** is constructed by connecting adjacent independent molecules via two Au(I) centers. The Au–Au distance for $(AuSPh)_2(\mu_2$-*t*-dpen) is 3.023(2) Å [14], which is just between that of the 2-*S*-pyridine derivative (**1**) (2.986(1) Å) and the 4-*S*-pyridine derivative (**2**) (3.239(2) Å). The Au–Au distance in **5** is 3.0840(6) Å, which is between 2.979(2) Å (**3**) and 5.8749(7) Å (**4**). The observation of an elongated Au–Au distance for **2** and **4** compared with the *S*-phenyl analogue $(AuSPh)_2(\mu_2$-*t*-dpen) and **5** is consistent with our previous conclusion that the aurophilicity is weak for the 4-*S*-pyridyl derivatives compared with the *S*-phenyl derivatives, although substitution of the SR group for Cl generally reinforces aurophilicity [8,16]. However, it is surprising to us that the 2-*S*-pyridyl group constricts the Au–Au separation strongly than the *S*-phenyl group and/or 4-*S*-pyridine. It is unlikely that the subtle difference of the electron donating ability between 2-*S*-pyridyl group and the 4-*S*-pyridyl group should induce such a dramatic change of the aurophilicity. Thus the following questions come out immediately, why 2-*S*-pyridine derivatives **1** and **3** exhibit such a strong aurophilic interaction, why not 4-*S*-pyridine derivative **4**? What is the most important factor to influence on the aurophilicity? Details on this query are described below and it seems appropriate to continue investigations into the effect of the carbon chain lengths on the aurophilicity at this moment. Systematic synthesis and X-ray structure analysis for diphosphines with C–C–C and C–C–C–C backbones have been attempted in order to assess the special role of 2-*S*-pyridyl group(s) on aurophilicity further. The crystal structures of **6** (the 2-*S*-py derivative with the C–C–C backbone) (Fig. 6(b)) and **7** (the *S*-Ph derivative with the C–C–C backbone) (Fig. 7(b)) show quasi one-dimensional chains which are constructed by connecting neighboring molecules through Au···Au interactions (r(Au–Au) = 3.1081(5) Å for **6** and 3.1389(5) Å for **7**). A similar quasi one-dimensional chain was reported previously for the starting chloride, but the Au–Au distance is significantly longer (r(Au–Au) = 3.316 Å) [17]. For the diphosphine ligand with the C–C–C backbone, the special role of the 2-*S*-pyridine on the aurophilicity is demonstrated again in **6**. However, the contribution of the 2-*S*-pyridine on the aurophilicity is not manifested in **8** where the carbon chain of the diphosphine ligand is C–C–C–C–. By substituting 4-*S*-pyridine for 2-*S*-pyridine, an analogous diphosphine derivative **9** is obtained; two neighboring molecules are aligned with a head to tail fashion to form parallelograms with an Au···Au contact of 3.626(1) Å in **9**. Although the observed Au–Au contact is slightly longer than the generally accepted distances for this interaction [6,11], the aggregation seems to be the result of this contact to some extent. Quite interestingly, the *S*-Ph analogue **10** with the same alkyl chain diphosphine ligand exhibits the aurophilicity (r(Au–Au) = 3.0926(5) Å). Two independent molecules of **10** are connected through Au–Au interactions to yield

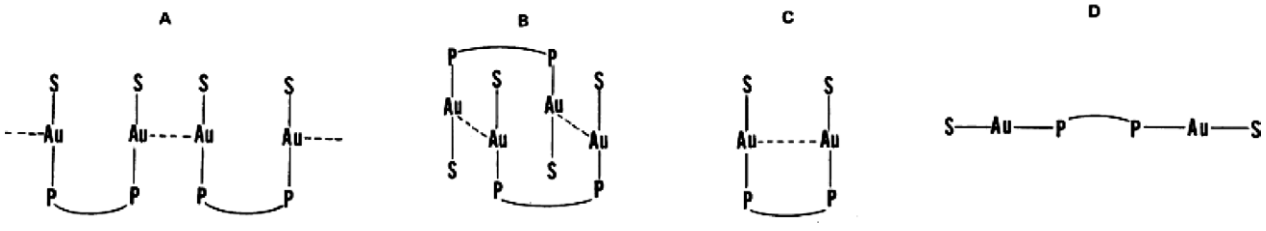

Chart 1. Structural motifs for diphosphine digold complexes.

a chain structure (Fig. 2(g)). The chains are parallel for each other in solid states. According to Balch et al. [12], no Au–Au interaction is observed for the parental chloride. Therefore, the effect of substituting SPh for Cl on the aurophilicity is evident for **10**. The comparison of the Au–Au distances in the present series of (Au-SR)$_2$(μ-diphosphine) derivatives and in those reported previously [13,14] indicates following two important trends. For the *S*-Ph series, the aurophilicity is less susceptible to the alkyl chain length in the diphosphine ligands up to C_4. However, the aurophilicity is quite sensitive to the alkyl chain length in the diphosphine ligands for the 2-*S*-pyridine series. From these trends, we were hit by an idea what happens on the aurophilicity by inserting a CH_2 group between the S and the pyridine ring. This idea was first examine by use of the simple triphenylphosphine derivatives. For **11** and **12**, no Au–Au interaction is induced by substituting 4-*S*-$(CH_2)_n$-py for Cl in the parental Ph_3P–Au–Cl [13,15]. Then we have examined the idea for [Au(4-*S*-CH_2-pyridine)]$_2$(μ-*t*-dpen). Our preliminary experiment shows a quite interesting result, that is, the insertion of a CH_2 group into the pyridine–S bond makes the Au–Au distance closer from 3.239(2) Å (**2**) to 3.102(3) Å [18]; this distance is shorter than that of $(AuCl)_2$dppe (r(Au–Au) = 3.189(1) Å) [16]. Solvent molecules sometimes play crucial role for the occurrence and/or strength of aurophilicity [10,12]. However, crystals of **1**–**5**, **7** and **9**–**12** do not contain solvent molecules. Bates et al. [16] and Balch and co-workers [12] have drawn attention to the change of aurophilic interaction due to the polymorphims in Au phosphine derivatives. Healy and co-workers [17] have also reported the importance of cooperative effects of weak forces in different crystal structures of the same Au compounds. We have also reported that the appearance of aurophilicity depends on the crystal polymorphism for simple mononuclear Au phosphine derivatives [13]. However, other crystal systems than those described in the present paper have not been detected so far for **1** and **3**. Thus 2-*S*-py ligand itself is important for the strong aurophilicity in **1** and **3**.

Balch et al. have indicated that there are some preferred geometrical parameters for Au–Au interaction in a series of $(AuX)_2\{P(CH_2)_nP\}$ derivatives [12]; the X–Au–Au–X torsional angles and X–Au–Au–Y angles average to 90°. For the present system where the A-type of aurophilicity is explicitly manifested, S–Au–Au–S torsional angles are 84.1°, 120.9°, 75.3°, and 64.6°, respectively for **1**, **3**, **4**, and **7**, P–Au–Au–P torsional angles are 77.6°, 121.3°, 71.0° and 67.3°, respectively, for this order, and S–Au–Au–P torsional angles are 99.2°, 59.7°, 104.7° and 109.0° and 114.0°, respectively, in this order. Observed Au–Au distances for the present series of compounds are generally shorter than those of Balch's chlorides but their trends do not hold for our compounds.

All of the available data mentioned above highlight the special role of the 2-*S*-pyridine ligand on the aurophilcity when the ligand is incorporated into the diphosphine ligands with short hydrocarbon backbone. One plausible explanation of the result is extended in the following section.

3.2. N···H–C= interaction and NMR spectra

In the above section, the special role of the 2-*S*-pyridine group on the aurophilicity was demonstrated in terms of the outlook of the molecular structure. In this section, the issue is discussed in terms of detailed X-ray and ^{1}H NMR data. Calculated crystal densities (Table 1) do not suggest that the crystal packing force is directly related to the strength of the aurophilicity. The ORTEP drawings of **1**, **3** and **4** (Fig. 1(a), 3(a) and 4(a)) have shown an interesting common feature at first glance; a quasi-coplanar structure is built up around the central part of each molecule including carbon and nitrogen atoms of the pyridine ring. The deviation of the H atom of the core CH–CH diphosphine from the best plane defined by the RS–Au–P–CH group is 0.80 Å for **1**, and 0.41 Å for **3**, respectively (calculations were made after the hydrogen positions were transferred by the symmetry operation). However, the deviation from the planarity is larger for **4**. In order to assess this coplanarity in another way, the dihedral angle between two planes (one is defined from the H–C1–P1–Au1–S1 array and the other is from the S–pyridine array) is calculated; the angle is 19.1(5)° for **1**, 21.9 (1)° for **3** and 35.8(1)° for **4**, respectively. The N···H–C angle is almost linear (157° for **1** and 173.5° for **3**, respectively) and the distance between N and observed H (from the Fourier map) is 2.8(2) Å [20]. These results suggest a kind of hydrogen bond between N and H–C– [20,21]. The lack of a hydrogen atom in an *ortho* position should make it possible for 2-*S*-pyridine rings to be coplanar with the C–P–Au–S backbone and small dihedral angles for **1** and **3** are thus rationalized. In **1** and **3**, the 2-*S*-pyridine ring and the S–Au–P–C moiety can provide a desired flat pedestal for N···H–C= interaction mentioned above. Thus N···H–C interaction is a certain viable source for this coplanarity. Aurophilicity has now been suggested to be quite sensitive to many factors, and the reported factors are sometime controversial [7,12,16,19]. Pyykkö has suggested that the ligand softness tends to reinforce the aurophilicity. The 2-*S*-pyridine group seems to play a similar role as a soft ligand at experimental levels; the S group at an *ortho*-position donates more electrons to Au(I) than that at the *para*-position. Further experiments to support possible N···H–C interaction are described below.

The ^{1}H NMR spectrum of **1** in $CDCl_3$ has shown that four magnetically different protons of 2-*S*-pyridyl ligand

Table 1
Crystal data

Compound	1	2	3	4	5	6	7	8	9	10	11	12
Chemical formula	$C_{36}H_{30}Au_2N_2P_2S_2$	$C_{36}H_{30}Au_2N_2P_2S_2$	$C_{36}H_{32}Au_2N_2P_2S_2$	$C_{36}H_{32}Au_2N_2P_2S_2$	$C_{38}H_{34}Au_2P_2S_2$	$C_{37}H_{34}Au_2N_2P_2S_2$	$C_{39}H_{36}Au_2P_2S_2$	$C_{44}H_{42}Au_2N_2P_2S_2$	$C_{38}H_{36}Au_2N_2P_2S_2$	$C_{40}H_{38}Au_2P_2S_2$	$C_{24}H_{21}Au_1N_1P_1S_1$	$C_{25}H_{23}Au_1N_1P_1S_1$
Formula weight	1010.7	1010.7	1012.7	1012.7	1010.8	1026.7	1024.7	1118.8	1040.7	1038.7	583.4	597.5
Crystal system	Monoclinic	Monoclinic	Monoclinic	Triclinic	Triclinic	Triclinic	Triclinic	Monoclinic	Triclinic	Triclinic	Triclinic	Triclinic
Space group	*C*2/*c*	*P*21/*n*	*C*2/*c*	$\bar{P}$	$\bar{P}$	$\bar{P}$	$\bar{P}$	$P2_1/n$	$\bar{P}$	$\bar{P}$	$\bar{P}$	$\bar{P}$
a (Å)	16.035(2)	16.691(5)	16.158(1)	8.759(2)	10.4706(9)	8.626(1)	8.718(2)	8.735(1)	9.918(1)	10.899(2)	9.070(6)	8.850(5)
b (Å)	20.323(2)	20.645(9)	19.762(1)	9.879(2)	11.636(1)	11.207(2)	11.637(3)	10.073(1)	9.910(1)	11.888(2)	11.309(7)	14.364(5)
c (Å)	11.264(4)	11.159(4)	11.214(1)	10.532(2)	16.468(2)	18.647(3)	17.863(4)	23.768(3)	19.098(1)	15.715(3)	11.536(9)	18.616(7)
α (°)	112.854(3)				70.771(2)	93.551(3)	92.446(3)		91.743(1)	107.380(3)	79.19(6)	75.90(3)
β (°)	114.33(1)	99.34(4)	111.744(1)	102.447(3)	86.757(2)	100.141(8)	93.144(4)	95.683(3)	88.221(1)	95.948(3)	71.30(5)	86.23(4)
γ (°)		90.409(3)			69.131(2)	107.408(5)	108.415(3)		74.900(1)	108.741(3)	89.61(5)	81.61(4)
V (Å^3)	3345.0(9)	3792(3)	3326.0(2)	815.9(2)	1765.9(3)	1680.5(4)	1713.4(2)	2080.8(5)	995.7(1)	1794.8(4)	1099(1)	2269(2)
Z	4	4	4	1	4	2	2	4	2	2	2	2
D_{calc} (g cm^{-3})	2.06	1.79	2.02	2.06	1.90	2.03	1.99	1.79	1.91	1.99	1.76	2.26
Crystal dimension (mm^3)	$0.55 \times 0.5 \times 0.3$	$0.75 \times 0.55 \times 0.45$	$0.1 \times 0.1 \times 0.1$	$0.15 \times 0.1 \times 0.1$	$0.1 \times 0.15 \times 0.1$	$0.1 \times 0.1 \times 0.1$	$0.1 \times 0.15 \times 0.1$	$0.2 \times 0.15 \times 0.1$	$0.1 \times 0.1 \times 0.1$	$0.1 \times 0.1 \times 0.1$	$0.6 \times 0.50 \times 0.45$	$0.7 \times 0.55 \times 0.40$
μ (mm)	9.02	7.94	12.3	9.24	8.5.	1.22	8.8	7.3	11.35	8.4.	6.9	6.8
Diffractometer	MXC3	MXC3	MAC DIP	SMART APEX	SMART APEX	MAC DIP	SMART APEX	SMART APEX	MAC DIP	SMART APEX	MXC3	MXC3
$2\theta_{max}$ (°)	50	45		55	55	55	55		55.0	50.0	45.0	
Temperature (K)	298	298	120	100	100	120	100	293	120	100	298	298
Unique reflections	2957	4954	7762	3558	7660	7681	4900	4775	10330	7855	3874	5941
Data reduction cut off	2355	3045	7222	3503	5485	6419	4542	2412	8749	7316	3117	5279
Number of parameter refined	203	227	263	205	260	406	550	235	559	501	253	293
R_1	0.064	0.102	0.02	0.04	0.08	0.04	0.03	0.06	0.04	0.04	0.096	0.098
wR_2	0.186	0.258	0.04	0.11	0.15	0.09	0.08	0.11	0.067	0.09	0.262	0.254

$R = \sum ||F_o| - |F_c|| / \sum |F_o|$; $Rw = \{\sum w[(F_o^2 - F_c^2)^2 / \sum w(F_o^2)^2]\}^{1/2}$, where $w = 1/[\sigma^2((F_o^2) + (ap)^2 + bp)]$.

appear as sharp signals at room temperature, suggesting that the solid state conformation about the *S*-pyridyl group is not fluxional on an NMR time scale even in a solution. In addition, the ethylene proton resonates at approximately 0.4 ppm lower field (δ 7.64) than that of $(AuSPh)_2(\mu_2$-*t*-dpen) [14]. Close contact between N and H–C= described above suggests that the lower field shift is the result of the hydrogen bond between N and H. If this is the case, the ethylene proton signal of **1** should be detected almost at the same position as those of aforementioned analogues, when the hydrogen bond formation is inhibited by blocking the N atom from this interaction. A drop of dilute hydrochloric acid suspension into $CDCl_3$was added to a NMR tube of **1**. After several hours standing, the mixture was subjected to ^{1}H NMR measurements; the addition caused a significant higher field shift of the ethylene proton (δ 7.52) with concomitant remarkable lower field shifts of pyridine proton signals, although peaks due to phenyl protons were left intact. The *ortho*-proton signal of the 2-*S*-pyridyl ligand was shifted from 7.37 to 7.38 (d) to 7.48, *meta*-proton signal(d) from 8.04 and 6.82 to 8.10 and 6.94, respectively, and the *para*-proton signal from 7.32 (t) to 7.43. We suspected at first that (Au–2–S–py)(Au–Cl)(μ_2-*t*-dpen) and/or $(AuCl)_2(\mu_2$-*t*-dpen) was yielded upon addition of HCl [14]. However, the observed ^{1}H NMR spectrum is entirely different from the spectra of these compounds. Therefore, the observed results are interpreted in terms that the lower-field shifts of pyridine protons are induced by the protonation of the N atom in the 2-*S*-pyridine ligand and the formation of the pyridinium salt is completed within several hours upon addition of hydrochloric acid, because no pyridine proton signal due to original **1** is detected. Another attempt to intervene such a hydrogen bonding is a use of pyridine as a solvent. However, such an attempt to take a ^{1}H NMR spectrum of **1** in deuterated pyridine was hampered because of low solubility in this solvent. We surmise that some kind of such an attractive force is effective even in solutions and co-planarity of the ethylene protons in the =CH–P group to the –S–pyridine-ring may be a good reason to account for a lower-field shift of this proton. Perhaps a kind of delocalized system (Scheme 1) is constructed and a ring current produced in these complexed rings is largely responsible for a lower field shift of the ethylene protons in **1**.

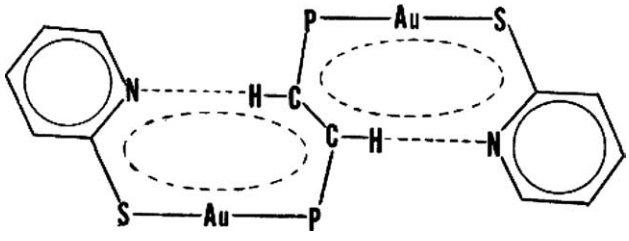

Scheme 1. Structural motifs for diphosphine digold complexes.

Jeffrey has classified hydrogen bonds into three categories, that is, strong, moderate and weak [21]. The general N···H interactions have been well documented and similarly classified [22]. Thaimattam et al. have reported that 4,4′-dicyanobiphenyl forms a 1:1 complex with urea via long C–H···N interactions (2.88 and 2.83 Å) and concluded that these interactions contribute in some measure to overall crystal and supra structural stabilization [23]. Among many examples where pyridyl and/or nucleotide N atoms are concerned, the observed N···H–C= contact in **1** seems to be an upper limit of weak interactions. Because of paucity of data, we do not intend to allege that this N···H–C= interaction reinforce the aurophilicity, but we propose that the findings should not be vitiated.

4. Conclusion

It is worth pointing that the 2-*S*-pyridine group is one of the best SR ligand to reinforce the aurophilicity for Au(I) diphosphine derivatives with a short hydrocarbon backbone. The 2-*S*-pyridine ring is almost coplanar to the P–C=C–P skeleton. The lack of the hydrogen atom on N makes this conformation possible and this leads to a kind of N···H–C= hydrogen bond. The compactness around the central part including Au, S, P, and the hydrocarbon backbone should be the most important factor to accentuate the aurophilicity.

5. Experimental

5.1. General comments

Reactions were carried out under an argon atmosphere by standard Schlenk techniques. The reaction vessel was covered with a piece of black cloth to shield from room light. All diphosphine ligands except *t*-dpen were purchased from Aldrich and Strem Chemicals Inc.; *t*-dpen was purchased from Tokyo Kasei Co. Ltd. 2- and 4-Pyridinethiols were also purchased from Aldrich. 4-Pyridineethanethiol was obtained from Tokyo Kasei Co. Ltd. in a form of hydrochloride. 4-Pyridinemethanethiol was synthesized according to the literature method with major revisions [24]. 4-Pyridinemethanethiol was kept in a form of dilute THF solution, because pure 4-pyridinemethanethiol decomposes easily.

^{1}H NMR spectra were recorded on a Varian Gemini-2000 (300 MHz) spectrometer and ^{31}P{^{1}H} NMR spectra were recorded at 80.984 MHz on a Varian XL-200 spectrometer. ^{31}P{^{1}H} NMR chemical shifts are referenced to external 85% H_3PO_4. C, H, N analyses were made for key compounds; characterizations of other compounds were done by ^{1}H NMR and single crystal X-ray diffractions.

5.2. Synthesis of [Au(x-S-pyridine)]$_2$(μ_2-t-dpen)

The synthesis of [Au(2-*S*-pyridine)]$_2$(μ_2-*t*-dpen) (**1**) (*t*-dpen = 1,2-bis(diphenylphosphino)-ethylene) described below was a typical procedure for [Au(*x*-*S*-pyridine)]$_2$(μ_2-diphos) type compounds. 2-*S*- and/or 4-*S*-pyridine group was introduced into $(AuCl)_2(\mu_2$-*t*-den) scaffold [13,25] by substituting $C_5H_4NS^-$ for Cl. In a 200-ml three necked round-bottom flask, a methanol solution (40 ml) of 2-pyridinethiol (120 mg, 1.25 mmol) and KOH (70 mg, 1.25 mmol) were placed and then a CH_2Cl_2 solution (50 ml) of $(Cl–Au)_2(\mu_2$-*t*-dpen) (430 mg, 0.50 mmol) was added. The mixture was stirred at room temperature overnight. Solvents were distilled off by rotary-evaporator to leave a pale yellow solid. The solid was washed with small amount of hexane, benzene and methanol successively. The residue was extracted with small amount of CH_2Cl_2 and was recrystallized from CH_2Cl_2–hexane to afford pale yellow crystals of **1**. Yield 330 mg, 65%. ^{31}P NMR: δ 36.2. ^{1}H NMR ($CDCl_3$, 300 MHz): δ 8.04 (d, 6-H in py, 2H), 7.64 (t, 18.6 Hz, HC═, 2H), 7.54–7.83 (m, PPh, 20H), 7.38-7.37 (d, 3-H in py, 2H), 7.32 (t, 4-H in py, 2H), 6.82 (t, 2-H in py, 2H). Anal. Calc. for $C_{36}H_{30}Au_2N_2P_2S_2$: C, 42.78; H, 2.99; N, 2.77. Found: C, 42.54; H, 2.76; N 2.62%.

The 4-pyridine-*S* analogue, [Au(4-*S*-pyridine)]$_2$(μ_2-*t*-dpen) (**2**) was obtained in 45% yield. ^{31}P NMR: δ 35.5. ^{1}H NMR ($CDCl_3$, 300 MHz): δ 8.13 (dd, 2,6-H in py, 4H), 7.50–7.66 (m, PPh, 20H), 7.40 (dd, 3,5-H in py, 4H), 7.25 (t, 19.2 Hz, HC═, 2H).

5.3. Synthesis of [Au(x-S-pyridine)]$_2$(μ_2-diphos)

[Au(2-*S*-pyridine)]$_2$(μ_2-dppe) (**3**) (dppe = 1,2-bis(diphenylphosphinoethane)) was similarly synthesized as above. 2-*S*- and/or 4-*S*-pyridine group was introduced into $(AuCl)_2(\mu_2$-diphos) scaffold [13,24] by substituting $C_5H_4NS^-$ for Cl. To a CH_2Cl_2 solution (20 ml) of $(AuCl)_2(\mu_2$-dppe) (86 mg, 0.1 mmol) was added 22 mg (0.2 mmol) of 2-pyridinethiol and 400 mg (3.8 mmol) of Na_2CO_3. The mixture was stirred at room temperature overnight and the solution was concentrated to 5 ml and to this was added 15 ml of diethylether. The mixture was left standing at room temperature for 24 h. The resulting yellow precipitates were collected on a frit and washed with small amount of diethylether to afford 68 mg (67%) of [Au(2-*S*-pyridine)]$_2$(μ_2-dppe) (**3**). Compound **3** was recrystallized from CH_2Cl_2–hexane to afford pale yellow crystals. ^{31}P NMR: δ 37.3 (s). ^{1}H NMR ($CDCl_3$, 300 MHz): δ 8.14–8.07 (m, 6-H in Spy, 2H), 7.84–7.70 (m, *o*-Ph, 8H), 7.53–7.40 (m, *m*-Ph, *p*-Ph, 3-H in Spy, 14H), 7.37–7.29 (m, 5-H in Spy, 2H), 6.86–6.77 (m, 4-H in Spy, 2H), 2.85 (s, –CH_2–, 4H). Anal. Calc. for $C_{36}H_{32}Au_2N_2P_2S_2$; C, 42.72; H, 3.19; N, 2.77. Found: C, 42.47 ; H, 3.00; N 2.78%.

The 4-*S*-pyridine analogue, [Au(4-*S*-pyridine)]$_2$(μ_2-dppe)(**4**), was similarly synthesized in 71% yield. ^{31}P NMR: δ 36.3 (s). ^{1}H NMR ($CDCl_3$, 300 MHz): δ 8.17–8.06 (m, 2,6-Spy, 4H), 7.72–7.58 (m, *o*-Ph, 8H), 7.57–7.38 (m, *m*-Ph, *p*-Ph, 3,5-H in Spy, 16H), 2.73 (s, –CH_2–, 4H).

The S-phenyl analogue, [Au(*S*-phenyl)]$_2$(μ_2-dppe) (**5**), was similarly synthesized in 76% yield. ^{31}P NMR: δ 37.3 (s). ^{1}H NMR ($CDCl_3$, 300 MHz): δ 7.73–7.55 (m, *o*-Ph, *m*-S-Ph, 12H), 7.55–7.38 (m, *m*-Ph, *p*-S-Ph, 12H), 7.15–6.95 (m, *o*-S-Ph, *p*-S-Ph, 6H), 2.94–2.73 (m, –CH_2–C–CH_2–, 4H), 2.10–1.82 (m, C–CH_2–C–, 2H).

[Au(2-S-pyridine)]$_2$(μ_2-dppp) (**6**) $\cdot$ 1/2C_6H_6 (dppp = 1,3-bis(diphenyl phosphino) propane) was synthesized in 83% yield. ^{31}P NMR: δ 32.1 (s). ^{1}H NMR ($CDCl_3$, 300 MHz): δ 8.15–8.08 (m, *6*-H in Spy, 2H), δ 7.81–7.67 (m, *o*-Ph, 8H), 7.50–7.35 (m, *m*-Ph, *p*-Ph, 3-H in Spy 14H), 7.35–7.27 (m, 5-H in Spy, 2H), 6.84–6.75 (m, 4-H in Spy, 2H), 3.09–2.90 (m, CH_2–C–CH_2, 4H), 2.16–1.92 (m, C–CH_2–C). [Au(S-phenyl)]$_2$(μ_2-dppp) (**7**) was similarly synthesized in 76% yield. ^{31}P NMR: δ 32.5 (s). ^{1}H NMR ($CDCl_3$, 300 MHz): δ 7.71–7.49 (m, *o*-Ph, *m*-S-Ph, 12H), 7.49–7.35 (m, *m*-Ph, *p*-Ph, 10H), 7.15–6.95 (m, *o*-S-Ph, *p*-S-Ph, 6H), 2.94–2.73 (m, CH_2–C–CH_2, 4H), 2.10–1.82 (m, C–CH_2–C). Anal. Calc. for $C_{37}H_{34}Au_2N_2P_2S_2 \cdot 1/2C_6H_6$; C, 45.08; H,3.50; N, 2.63. Found: C, 45.06; H, 3.60; N, 2.60%.

The 2-*S*-pyridine analogue [Au(2-*S*-pyridine)]$_2$(μ_2-dppb) (dppb = 1,4-bis(diphenyl phosphino)butane) (**8**) was similarly synthesized in 58% yield. ^{31}P NMR: δ 34.71 (s). ^{1}H NMR ($CDCl_3$, 300 MHz): δ 8.24–8.18 (m, 6-S-py, 2H), 7.78–7.65 (m, *o*-Ph, 8H), 7.52–7.38 (m, *m*-Ph, *p*-Ph, 5-H in Spy, 14H), 7.36–7.29 (m, 5-H in Spy, 2H), 6.88–6.79 (m, 4-H in Spy, 2H), 2.77–2.38 (m, –CH_2–C–C–CH_2–, 4H), 1.98–1.80 (m, –C–CH_2–CH_2–C–, 4H). Anal. Calc. for $C_{38}H_{36}Au_2N_2P_2S_2$; C, 43.86; H, 3.49; N, 2.69. Found: C, 43.95; H, 3.51; N, 2.64%.

[Au(4-*S*-pyridine)]$_2$(μ_2-dppb) (**9**) was similarly synthesized in 72% yield. ^{31}P NMR: δ 35.1 (s). ^{1}H NMR ($CDCl_3$, 300 MHz): δ 8.18–8.14 (m, 2,6-S-py, 4H), 7.72–7.58 (m, *o*-Ph, 8H), 7.56–7.42 (m, *m*-Ph, *p*-Ph, 3,5-H in Spy, 16H), 2.58–2.37 (m, –CH_2–C–C–CH_2–, 4H), 1.93–1.76 (m, –C–CH_2–CH_2–C–, 4H). The *S*-phenyl analogue [Au(*S*-phenyl)]$_2$(μ_2-dppb) (**10**) was similarly synthesized in 74% yield. ^{31}P NMR: δ 35.10 (s). ^{1}H NMR ($CDCl_3$, 300 MHz): δ 7.72–7.54 (m, *o*-Ph, *m*-S-Ph, 12H), 7.54–7.40 (m, *m*-Ph, *p*-Ph, 12H), 7.16–6.94 (m, *o*-S-Ph, *p*-S-Ph, 6H), 2.58–2.38 (m, –CH_2–C–C–CH_2–, 4H), 1.95–1.75 (m, –C–CH_2–CH_2–C–, 4H).

5.4. Synthesis of Au{4-S-$(CH_2)_n$-pyridin}PPh_3

The synthesis of Au(4-*S*-CH_2-pyridine)PPh_3 (**11**) described below was a typical procedure for this type of

compounds. To a 300 ml three necked round-bottom flask, a CH_2Cl_2 solution (100 ml) of Ph_3PAuCl (156 mg, 0.32 mmol) was added. Then a methanol solution (70 ml) which contains 100 mg (0.8 mmol) of 4-pyridinemethanethiol and 20 mg (0.36 mmol) of KOH was dropped for 1.5 h. After the mixture was stirred at room temperature for 3 h, the solvent was rotary-evaporated and the resulting pale yellow solid was recrystallized from CH_2Cl_2/hexane (1:1) two give very pale yellow crystals of **11** in 81% yield. ^{31}P NMR: δ 37.29 (s). ^1H NMR ($CDCl_3$, 300 MHz): δ 8.37 (d, 2, 6-H in Spy, 2H), 7.75 (d, 3, 5-H in Spy, 2H), 7.39–7.56 (m, Ph, 15H), 4.21 (s, $-CH_2-$, 2H).

Au{4-*S*-$(CH_2)_2$-pyridine}PPh_3 (**12**) was synthesized similarly from Ph_3PAuCl (1.00 g, 2 mmol), 365 mg (2 mmol) of 4-pyridineethanethiol hydrochloride, and 175 mg (3 mmol) of KOH. Yield of **12** is 1.14 g (95%). ^{31}P NMR: δ 36.88 (s). ^1H NMR ($CDCl_3$, 300 MHz): δ 8.36 (dd,, 2,6-H in Spy, 2H), 7.53–7.44 (m, Ph, 15H), 7.13 (d, 3,5-H in Spy, 2H), 3.31 (t, S–CH_2-, 2H), 3.02 (t, S–C–CH_2-py, 2H).

5.5. X-ray crystallography

Crystals suitable for X-ray studies were generally grown from CH_2Cl_2–hexane solutions. Selected crystals of **1**, **2**, **11** and **12** were glued to the top of a fine glass rod and the reflection data were collected at room temperature on a MAC MXC3 diffractometer with graphite monochromated Mo Kα radiation (λ = 0.71073 Å). Reflection data for **4**, **5**, **7**, **8** and **10** were collected at 100 K on a Bruker SMART-APEX CCD diffractometer with graphite-monochromated Mo Kα radiation (λ = 0.71073 Å); these crystals were mounted on a nylon loop. The SPring-8 BL04B2 beam line (λ = 0.3282 Å) equipped with a MAC DIP-LABO imaging plate diffractometer [26] was used for data collections of **3**, **6** and **9** at 120 K because only small size crystals were available for these compounds; these crystals were attached on a nylon loop similarly as above. The structures of these crystals were solved by the direct method using SIR-97 in a WINGX program package and refined with anisotropic displacement parameters by full-matrix least-squares with SHELXS-97 in a WINGX program package [27]. Carbon atoms in Ph and S-py groups for **1**, **2**, **11** and **12** were refined isotropically, because numbers of these atoms have a negative thermal factors upon anisotropic refinements; crystals of these compounds are liable to decompose during reflection data collection for several days and the data accumulated are not at a satisfactory level. The refinements were made on F^2 data and the final R and wR_2 values are given in Table 1. Tables for atomic coordinates, displacement parameters, and bond-lengths and angles are available as supplementary materials. Selected bond lengths and angles are given in Table 2. The supplementary crystallographic data are contained in CCDC-240099 (**1**), -240100 (**2**), -240101 (**3**), -240102 (**4**),

Table 2
Selected bond lengths (Å) and angles (°)

Compound	1	2	3	4	5	6	7	8	9	10	11	12
Bond distances (Å)												
Au–Au	2.986(1)	3.239(2)	2.9679(2)		3.0840 (6)	3.1081(5)	3.1389(5)		3.626(1)	3.0926(5)		
Au–S	2.312(4)	2.29(1)	2.3087(4)	2.296(5)	2.296(5)	2.321(2)	2.321(2)	2.300(3)	2.311(1)	2.311(2)	2.294(8)	2.298(4)
		2.294 (9)			2.310(3)	2.320(2)	2.312(2)		2.314(1)	2.291(3)		2.292(4)
Au–P	2.260(4)	2.255(9)	2.2629(4)	2.253(2)	2.259(3)	2.262(2)	2.273(2)	2.248(3)	2.268(1)	2.259(2)	2.265(6)	2.258(4)
		2.258(8)			2.254(2)	2.259(2)	2.259(2)		2.269(1)	2.263(2)		2.276(4)
S–C	1.73(2)	1.74(4)	1.754(2)	1.756(7)	1.724(5)	1.753(7)	1.774(8)	1.74(2)	1.751(4)	1.771(6)	1.63(4)	1.90(2)
		1.73(3)			1.758(4)	1.73(1)	1.796(7)		1.745(4)	1.59(1)		1.79(2)
P–C	1.80(2)	1.77(3)	1.819(1)	1.815(5)	1.816(9)	1.829(7)	1.834(7)	1.82(2)	1.819(3)	1.830(6)	1.79(2)	1.86(2)
	1.83(2)	1.84(3)	1.812(1)	1.810(5)	1.799(4)	1.841(7)	1.807(7)	1.81(1)	1.821(4)	1.808(4)	1.75(3)	1.84(1)
	1.79(1)	1.82(3)	1.814(1)	1.797(6)	1.824(2)	1.805(7)	1.822(7)	1.84(1)	1.812(4)	1.817(7)	1.85(2)	1.82(1)
		1.83(3)			1.826(3)	1.806(9)	1.838(7)		1.811(4)	1.819(5)		1.81(1)
		1.88(3)			1.791(3)	1.795(8)	1.829(8)		1.826(4)	1.816(7)		1.83(2)
		1.84(3)			1.847(4)	1.809(7)	1.820(6)		1.822(4)	1.818(8)		1.87(1)
Bond angles (°)												
P–Au–S	176.8(1)	174.9(4)	176.80 (1)	174.91(7)	172.3(1)	173.36(7)	171.26(6)	175.9(1)	178.32(4)	174.73(5)	175.6(2)	178.5(2)
		172.8(4)			170.6(1)	172.16(7)	167.63(6)		178.33(4)	175.05(8)		175.3(2)
Au–S–C	108.9(6)	102(2)	108.74(4)	105.5(2)	105.3(2)	105.2(2)	108.2(2)	101.1(5)	108.9(1)	105.7(2)	120(3)	102.3(6)
		105(1)			99.3(2)	101.1(3)	96.2(2)		109.0(1)	112.3(5)		103.8(7)
Au–P–C	109.4(5)	114(1)	107.98(4)	114.5(2)	108.7(3)	114.0(3)	112.8(3)	109.5(4)	115.9(1)	113.6(2)	111.9(7)	109.0(4)
	118.9(5)	116(1)	115.6(4)	112.4(2)	117.1(2)	113.7(2)	112.6(2)	118.1(4)	113.4(1)	113.4(2)	114.0(7)	114.4(5)
	118.5(5)	111(1)	118.29(4)	113.1(2)	117.2(1)	114.3(3)	116.3(2)	114.2(3)	111.0(1)	110.4(2)	112(1)	114.8(5)
		112.8(9)			109.7(1)	112.2(2)	113.9(2)		116.2(1)	116.6(3)		113.2(5)
		110(1)			114.5(2)	112.2(2)	115.6(2)		111.0(1)	113.1(2)		113.6(4)
		115(1)			118.0(1)	115.8(2)	111.4(2)		113.6(1)	110.1(2)		114.5(5)
Au–Au–S	77.6(1)	85.3(3)	77.86(3)		80.13(8)	94.40(5)	92.02(4)			84.26(4)		
	73.9(1)	73.8(2)			79.85(8)	87.36(6)	94.30(5)			78.01(7)		
Au–Au–P	102.81(9)	101.6(2)	102.61(4)		105.27(6)	91.47(5)	96.70(5)			98.87(4)		
					106.91(6)	100.05(5)	98.02(5)			106.94(4)		
					103.2(1)		108.2(4)					

-240103 (**5**), -240104 (**6**), -240104 (**7**), -240105 (**8**), -240106 (**9**), -240107 (**10**), -240108 (**11**) and -240109 (**12**).

Acknowledgements

This research was funded by Grants-in Aid for Scientific research on Priority Area (No. 12023221 ''Metal-assembled Complexes'') and by Grants-in Aid for Scientific research (No. 14540514) from the Ministry of Education, Science, Sports and Culture, Japan. The synchrotron radiation experiment was performed at the BL04B2 beamline in the SPring-8 with the approval of the Japan Synchrotron Radiation Research Institute (JASRI) (Proposal No. 2002A0475-ND1-np, 2003A0454-CD1-np, 2003B0346-ND1b-np).

Thanks are also due to Professor Motohiro Nishio for his valuable discussions on hydrogen bonds.

References

[1] J.-M. Lehn, Supramolecular Chemistry, VCH, New York, 1995; B.J. Hilliday, C.A. Mirkin, Angew. Chem. Int. Ed. 40 (2001) 2023; D. Braga, F. Grepioni, A.G. Orpen (Eds.), Crystal Engineering : From Molecules and Crystals to Materials, Kluwer Academic Publishers, Dordrecht, 1999; L. Ouahab, Chem. Mater. 9 (1997) 1909, and references therein.
[2] R.J. Puddephatt, Coord. Chem. Rev. 216–217 (2001) 313.
[3] G. Schmid (Ed.), Clusters and Colloids, VCH, Weinheim, 1994, and references therein.
[4] H. Schmidbaur (Ed.), Gold, Wiley, Chichester, 1999, and references therein.
[5] L.S. Ahmed, W. Clegg, D.A. Davis, J.R. Dilworth, M.R.J. Elsegood, D.V. Griffiths, L. Horsburgh, J.R. Miller, N. Wheatley, Polyhedron 18 (1999) 593, and references therein.
[6] H. Schmidbaur, Chem. Soc. Rev. 210 (1995) 391, and references therein; A. Bauer, H. Schmidbaur, J. Am. Chem. Soc. 118 (1996) 5324; W. Schneider, A. Bauer, H. Schmidbaur, Organometallics 15 (1996) 5445; A. Sladek, K. Angermaier, H. Shmidbaur, J. Chem. Soc., Chem. Commun. (1996) 1959; C. Hollatz, A. Schier, H. Schmidbaur, J. Am. Chem. Soc. 119 (1997) 8115; M. Preisenberger, A. Bauer, A. Schier, H. Schmidbaur, J. Chem. Soc., Dalton Trans. (1997) 4753; A. Bayler, A. Bauer, H. Schmidbaur, Chem. Ber. 130 (1997) 130; W. Schneider, A. Bauer, H. Schmidbaur, J. Chem. Soc., Dalton Trans. (1997) 415.
[7] F. Canales, M.C. Gimeno, A. Laguna, P.G. Jones, J. Am. Chem. Soc. 118 (1996) 4839; E.J. Fernandez, J.M. Lopez-de-Luzuriaga, M. Monge, M.A. Rodriguez, O. Crespo, M.C. Gimeno, A. Laguna, P.G. Jones, Chem. Eur. J. 6 (2000) 636.
[8] S.-J. Shieh, X. Hong, S.-M. Peng, C.-M. Che, J. Chem. Soc., Dalton Trans. (1994) 3067; B.-C. Tzeng, W.-C. Lo, C.-M. Che, S.-M. Peng, J. Chem. Soc., Chem. Commun. (1996) 181; B.-C. Tzeng, K.-K. Cheung, C.-M. Che, J. Chem. Soc., Chem. Commun. (1996) 1681; B.-C. Tzeng, C.-M. Che, S.-M. Peng, J. Chem. Soc., Chem. Commun. (1997) 1771.
[9] R.M. Davila, R.J. Staples, J.P. Fackler Jr., Organometallics 13 (1994) 418; J.M. Forward, Z. Assefa, J.P. Fackler Jr., J. Am. Chem. Soc. 117 (1995) 9103; A. Burini, J.P. Fackler Jr., R. Galassi, B.R. Pietroni, R.J. Staples, J. Chem. Soc., Chem. Commun. (1998) 95.
[10] M.J. Irwin, L.M. Rendina, J.J. Vittal, R.J. Puddephatt, J. Chem. Soc., Chem. Commun. (1996) 1281; M.J. Irwin, J.J. Vittal, G.P.A. Yap, R.J. Puddephatt, J. Am. Chem. Soc. 118 (1996) 13101.
[11] P. Pykkö, J. Li, N. Runeberg, Chem. Phys. Lett. 218 (1994) 133; P. Pykkö, J. Li, N. Runeberg, F. Mendizabal, Chem. Eur. J. 3 (1997) 1451; P. Pykkö, F. Mendizabal, Chem. Eur. J. 3 (1997) 1458, and references therein.
[12] P.M.V. Calcar, M.M. Olmstead, Al.L. Balch, J. Chem. Soc., Chem. Commun. (1995) 1773; P.M.V. Calcar, M.M. Olmstead, Al.L. Balch, Inorg. Chem. 36 (1997) 5231.
[13] K. Nunokawa, S. Onaka, T. Tatematsu, M. Ito, J. Sakai, Inorg. Chim. Acta 322 (2001) 56.
[14] S. Onaka, Y.. Katsukawa, M. Shiotsuka, O. Kanegawa, M. Yamashita, Inorg. Chim. Acta 312 (2001) 100.
[15] T. Yoshida, S. Onaka, M. Shiotsuka, Inorg. Chim. Acta 342 (2003) 319.
[16] According to Bates et al., Au–Au distance in the parental $(AuCl)_2$dppe is 3.189(1) Å . Eggleston et al. demonstrated that the parental chloride possesses two polymorphic crystal forms and both crystal forms exhibit intermolecular Au–Au interaction (3.187(1) and 3.221(1) Å, respectively); P.A. Bates, J.M. Waters, Inorg. Chim. Acta 98 (1985) 125; D.S. Eggleston, D.F. Chodosh, G.R. Girard, D.T. Hill, Inorg. Chim. Acta 108 (1985) 221.
[17] M.K. Cooper, L.E. Mitchell, K. Henrick, M. McPartlin, A. Scott, Inorg. Chim. Acta 84 (1984) L9.
[18] S. Onaka, M. Horibe, K. Nunokawa, to be published.
[19] R.C. Bott, P.C. Healy, G. Smith, Aust. J. Chem. 57 (2004) 213.
[20] For **1**, two program systems CRYSTAN and/or CRYSTAN-GM and SHELXS-97 were used. This distance was obtained from the least-squares refinements on *F* by use of Crystan program[13].
[21] G.A. Jeffrey, An Introduction to Hydrogen Bonding, Oxford University Press, 1997, and references therein.
[22] G.R. Desiraju, T. Steiner, The Weak Hydrogen Bond, Oxford Science Publications, 1999, and references therein.
[23] R. Thaimattam, D.S. Reddy, F. Xue, T.C.W. Mac, A. Nagia, G.R. Desiraju, J. Chem. Soc., Perkin Trans. 2 (1998) 1783.
[24] A. Fischer, M.J. King, F.P. Robinson, Can. J. Chem. 56 (1978) 3072.
[25] C.A. McAuliffe, R.V. Parish, P.D. Randall, J. Chem. Soc., Dalton Trans. (1979) 1730.
[26] T. Ozeki, K. Kusaka, H. Honma, Y. Nakamura, S. Nakamura, S. Oike, N. Yasuda, H. Imura, H. Uekusa, M. Isshiki, C. Katayama, Y. Ohashi, Chem. Lett. (2001) 804.
[27] G.M. Sheldrick, SHELX-97, University of Göttingen, Germany, 1997.